AIAA JOURNAL
Vol. 33, No. 6, June 1995

Buckling Mode Localization in Randomly Disordered Multispan Continuous Beams

Wei-Chau Xie*
University of Waterloo, Waterloo, Ontario N2L 3G1, Canada

Buckling mode localization in large randomly disordered multispan continuous beams is studied. When the cross-sections of each span are uniform, an exact formulation is employed to establish the equations of equilibrium in terms of the angles of rotations at the supports. When the cross-sections of each span are not uniform, a finite element method is applied to set up the governing equations. Two approaches are applied to determine the localization factors, which characterize the average exponential rates of growth or decay of amplitudes of deformation. The first method applies a transfer matrix formulation and Furstenberg's theorem on the asymptotic behavior of products of random matrices. The second method uses a Green's function formulation for a linear eigenvalue problem of a block tridiagonal form.

Nomenclature

EI	= average flexural rigidity of spans or elements
EI_i	= flexural rigidity of span i with uniform cross sections
EI_{ij}	= flexural rigidity of element j in span i
G_{ij}	= Green's function
$\boldsymbol{K}$	= stiffness matrix of an N-span continuous beam
$\boldsymbol{K}^G$	= geometric stiffness matrix of an N-span continuous beam
$\boldsymbol{K}_i^s$	= stiffness matrix of span i
$\boldsymbol{K}_i^{G,s}$	= geometric stiffness matrix of span i
k	= average flexural stiffness of spans, EI/L
k_i	= flexural stiffness of span i, EI_i/L_i
L	= average length of spans
L_i	= length of span i with uniform cross sections
L_{ij}	= length of element j in span i
l	= average length of elements
l_{ij}	= L_{ij}/l
M	= number of finite elements in each span
N	= number of spans
P	= compressive axial load
P_E	= Euler buckling load for a simply supported beam of length L and flexural rigidity EI, $EI(\pi/L)^2$
r_{ij}	= $1/l_{ij}$
s, c	= stability functions
$\boldsymbol{T}_i$	= transfer matrix
T_i	= torsional spring stiffness at support i
t_i	= T_i/k
$\boldsymbol{u}_i$	= nondimensional displacement vector of span i
θ_i	= angle of rotation at support i
κ_{ij}	= $2(l/L_{ij})^3(EI_{ij}/EI)$
λ	= Lyapunov exponent, localization factor
ν	= $\pi^2\rho/(30M^2)$
ρ	= P/P_E

I. Introduction

In practice, many structures are designed to be composed of identically constructed elements which are assembled end to end to form a large spatially periodic structure. However, due to defects in manufacture and assembly, no structure designed as a periodic structure can be perfectly periodic. Disorder can occur in the geometry of configurations and material properties of the structure and is generally of a random nature.

If a structure is perfectly periodic, the vibration modes are of wavy shapes and extend throughout the structure. However, if it is randomly disordered, the vibration will be confined to a small region with the amplitudes decaying exponentially away from a center. This phenomenon is called vibration mode localization. It is, therefore, important to evaluate the localization factors, the average exponential rates at which the amplitudes of vibration grow or decay. The reciprocal of the localization factor is the localization length, which characterizes the distance that vibration can extend.

The study of the localization phenomenon in randomly disordered systems has been an active area of research in solid state physics for the last three decades. Ishii[1] applied Furstenberg's theorem[2] on the limiting behavior of products of random matrices to study localization in one-dimensional systems such as random mass-spring chains. Using a Green's function formulation, Herbert and Jones,[3] and Thouless[4] were able to obtain the expression for the localization factor in terms of the density of states. The most important feature of one-dimensional disordered systems is that almost all states are localized.

Hodges[5] was the first to explain vibration localization in engineering structures by the example of an array of coupled oscillators or pendula whose natural frequencies vary from site to site. Since then there have been several studies on the localization in vibration modes of structures. In a series of publications[6–8] and the references therein, localization in vibration modes for monocoupled disordered structural systems was studied.

Most of the research on mode localization has been on vibration modes; few works have been done on localization in buckling modes of large disordered periodic structures. Pierre and Plaut[9] studied buckling mode localization for a two span continuous beam under axial compressive load in which the lengths of the two spans are different. In the present paper, the localization in buckling modes of large randomly disordered nearly periodic multispan continuous beams is studied. It is well known that a long continuous beam over many simple supports of equal span subject to axial compression will lose its stability in the straight configuration when the axial load is equal to one of the buckling loads. The buckling modes are of wavy shapes and extend throughout the structure. Similarly, a ring-stiffened circular cylindrical shell under axial compression may theoretically lose its stability by the formation of wavy shapes occurring longitudinally between the stiffeners and over the circumference, which extend throughout the cylinder. However, in many experimental studies of the buckling of ring-stiffened shells, only localized buckling modes were observed.[10,11] For strong ring-stiffened shells, two or three buckles at most would emerge when the critical load was reached; buckles occurred only in one bay. For weak ring-stiffened shells, buckles appeared around the whole circumference but extended throughout only a few bays. If each bay is considered as an element of the periodic structure, the localized buckles may be explained by the theory of localization in randomly disordered systems, since in reality the bays can never be identical but will be disordered in some random fashion.

Received Oct. 6, 1994; revision received Jan. 23, 1995; accepted for publication Jan. 23, 1995.

*Assistant Professor, Solid Mechanics Division, Faculty of Engineering.

In this paper, the phenomenon of buckling mode localization in disordered multispan continuous beams with uniform sections is studied in Sec. II using an exact formulation. If the cross sections within each span of the continuous beam are not uniform, such as those in long bridge structures, there is no exact formulation available; approximate methods have to be applied. In Sec. III, a finite element formulation and the method of condensation are applied to establish the equations of equilibrium of continuous beams with nonuniform sections. The localization factors of buckling modes under axial compressive loads are related to the larger one of the two Lyapunov exponents of the corresponding random discrete dynamical systems. Furstenberg's theorem[2] on asymptotic properties of products of random matrices is applied to evaluate the localization factors. As an alternative method, the localization factors are also obtained using the method of Green's function.

II. Buckling Mode Localization in Multispan Beams with Uniform Cross Sections

An N-span continuous beam under compressive load P as shown in Fig. 1 is considered. The length of the ith span is L_i, and the flexural stiffness is $k_i = EI_i/L_i$. The average span length and flexural stiffness are L and k, respectively. The torsional spring connecting span $i-1$ and span i has spring stiffness T_i, which reflects the coupling between these two spans. When T_i is small, span $i-1$ and span i are strongly coupled, whereas when T_i is large, the two spans are weakly coupled. As an extreme case, when T_i approaches infinity, each span is individually clamped; there is no coupling between the adjacent spans.

Consider a beam of length L and flexural stiffness $k = EI/L$ as shown in Fig. 2. It is known that[12] to have a rotation θ at support A and no rotation at support B, a moment $M_A = sk\theta$ at support A and a moment $M_B = sck\theta$ at support B are required, where s and c are the stability functions defined as

$$s = \frac{(1-2\alpha\cot 2\alpha)\alpha}{\tan\alpha - \alpha}, \quad c = \frac{2\alpha - \sin 2\alpha}{\sin 2\alpha - 2\alpha\cos 2\alpha}, \quad \alpha = \frac{\pi}{2}\sqrt{\rho}$$

Assume that, for the N-span continuous beam as shown in Fig. 1, the rotation at support i is θ_i. Employing the preceding result, the equilibrium condition at support i requires

$$s_{i-1}c_{i-1}k_{i-1}\theta_{i-1} + (s_{i-1}k_{i-1} + s_i k_i + T_i)\theta_i + s_i c_i k_i \theta_{i+1} = 0 \quad (1)$$

where

$$s_i = \frac{(1-2\alpha_i\cot 2\alpha_i)\alpha_i}{\tan\alpha_i - \alpha_i}, \qquad c_i = \frac{2\alpha_i - \sin 2\alpha_i}{\sin 2\alpha_i - 2\alpha_i\cos 2\alpha_i}$$

$$\alpha_i = \frac{\pi}{2}\sqrt{\rho_i}, \quad \rho_i = \frac{P}{P_{E,i}} = \frac{\rho}{\hat{\rho}_i}, \quad \hat{\rho}_i = \frac{P_{E,i}}{P_E}$$

$$P_{E,i} = EI_i(\pi/L_i)^2$$

From Eq. (1), θ_{i+1} may be expressed as

$$\theta_{i+1} = -\frac{s_{i-1}\hat{k}_{i-1} + s_i\hat{k}_i + t_i}{s_i c_i \hat{k}_i}\theta_i - \frac{s_{i-1}c_{i-1}\hat{k}_{i-1}}{s_i c_i \hat{k}_i}\theta_{i-1}$$

$$i = 2, 3, \ldots, N$$

where $\hat{k}_i = k_i/k$, $t_i = T_i/k$, or in the matrix form,

$$\boldsymbol{x}_i = \boldsymbol{T}_i\boldsymbol{x}_{i-1}, \qquad \boldsymbol{x}_i = \begin{Bmatrix} \theta_{i+1} \\ \theta_i \end{Bmatrix}$$

$$\boldsymbol{T}_i = \begin{bmatrix} -\dfrac{s_{i-1}\hat{k}_{i-1} + s_i\hat{k}_i + t_i}{s_i c_i \hat{k}_i} & -\dfrac{s_{i-1}c_{i-1}\hat{k}_{i-1}}{s_i c_i \hat{k}_i} \\ 1 & 0 \end{bmatrix} \quad (2)$$

in which $\boldsymbol{T}_i$ is the transfer matrix. The state vector $\boldsymbol{x}_n = \{\theta_{n+1}, \theta_n\}^T$ can be related to the initial state vector $\boldsymbol{x}_1 = \{\theta_2, \theta_1\}^T$ by a product of transfer matrices $\boldsymbol{x}_n = \boldsymbol{T}_n\boldsymbol{T}_{n-1}\cdots\boldsymbol{T}_2\boldsymbol{x}_1$, where the superscript T denotes transpose.

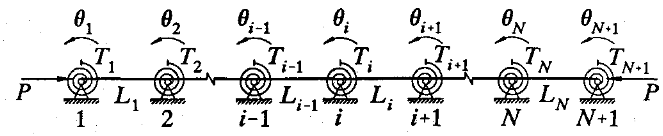

Fig. 1 Multispan continuous beam under compressive axial load.

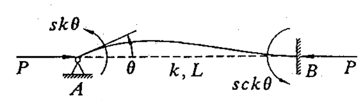

Fig. 2 Stability functions s and c.

It is assumed that the disorders of spans are random, independent of other spans, and have a common probability distribution. Then, the transfer matrices $\boldsymbol{T}_i$ will also be independent and identically distributed. The rate of growth of the state vector $\boldsymbol{x}_n$ or θ_{n+1} is governed by the behavior of the product of random matrices $T_n T_{n-1}\cdots T_2$. The asymptotic properties of such a product have been studied by many researchers. In this paper, Furstenberg's theorem[2] on the limiting behavior of products of random matrices will be utilized. Furstenberg's theorem may be stated as follows.

Furstenberg's Theorem. Let $\boldsymbol{T}_1, \boldsymbol{T}_2, \ldots, \boldsymbol{T}_n$ be nonsingular, independent, identically distributed 2×2 matrices, where $\boldsymbol{T}_i = \boldsymbol{T}_i(\epsilon)$ is a function of the random vector ϵ with probability density $p(\epsilon)$. If at least two of the random transfer matrices do not have common eigenvectors, and if

$$\lim_{n\to\infty}\frac{1}{n}\ell n\left(\prod_{i=1}^{n}|\det\boldsymbol{T}_i|\right) = 0 \quad (3)$$

then there exists a constant $\lambda > 0$ such that, for each $\boldsymbol{x}_0 \neq 0$,

$$\lim_{n\to\infty}\frac{1}{n}\ell n\|\boldsymbol{T}_n\boldsymbol{T}_{n-1}\cdots\boldsymbol{T}_1\boldsymbol{x}_0\| = \lambda \quad (4)$$

with probability 1, and

$$\lim_{n\to\infty}\frac{1}{n}\ell n\|\boldsymbol{T}_n\boldsymbol{T}_{n-1}\cdots\boldsymbol{T}_1\| = \lambda \quad (5)$$

with probability 1, where $\|\boldsymbol{x}\|$ is a suitable norm of the vector $\boldsymbol{x}$, and $\|\boldsymbol{T}\|$ denotes a suitable norm of the matrix $\boldsymbol{T}$.

It can easily be seen that the transfer matrices defined in Eq. (2) satisfy the condition (3). Applying Furstenberg's Theorem to Eq. (2), one obtains, with probability 1,

$$\lim_{n\to\infty}\frac{1}{n-1}\ell n\|\boldsymbol{x}_n\| = \lim_{n\to\infty}\frac{1}{n-1}\ell n\|\boldsymbol{T}_n\boldsymbol{T}_{n-1}\cdots\boldsymbol{T}_2\boldsymbol{x}_1\| = \lambda > 0$$

implying that, for large n,

$$\|\boldsymbol{x}_n\| = e^{\lambda(n-1)}\|\boldsymbol{x}_1\| \quad (6)$$

The positive number λ characterizes the average exponential rate of growth of the norm of the state vector $\boldsymbol{x}_n = \{\theta_{n+1}, \theta_n\}^T$; λ is called the Lyapunov exponent. It can be shown that Eq. (6) implies for large n

$$|\theta_{n+1}| = e^{\lambda n}|\theta_1| \quad (7)$$

Therefore, the Lyapunov exponent λ characterizes the exponential rate of growth of the angles of rotations. The positivity of the Lyapunov exponent λ for randomly disordered structure results in the localization in the buckling modes, since the nonzero angles of rotation growing exponentially from each end of the large multispan beam must match at the maximum; in other words, the buckling mode is localized with amplitudes decaying exponentially at the average rate λ on either side of some region. The Lyapunov exponent λ is, therefore, the localization factor.

On the other hand, letting $\boldsymbol{B}_n = \boldsymbol{T}_n\boldsymbol{T}_{n-1}\cdots\boldsymbol{T}_2$, one obtains $\boldsymbol{x}_n = \boldsymbol{B}_n\boldsymbol{x}_1$. The Euclidean norm of $\boldsymbol{x}_n$ is $\|\boldsymbol{x}_n\|^2 = \boldsymbol{x}_1^T\boldsymbol{B}_n^T\boldsymbol{B}_n\boldsymbol{x}_1$. Let $\sigma_{\max}^2 = \sigma_1^2 \geq \sigma_2^2 = \sigma_{\min}^2$ be the eigenvalues of $\boldsymbol{B}_n^T\boldsymbol{B}_n$, and $\boldsymbol{e}_1$

and e_2 the corresponding orthonormal eigenvectors. By Rayleigh's principle

$$\sigma_{\max}^2 = \frac{e_1^T B_n^T B_n e_1}{\|e_1\|^2} \geq \frac{x_1^T B_n^T B_n x_1}{\|x_1\|^2} \geq \frac{e_2^T B_n^T B_n e_2}{\|e_2\|^2} = \sigma_{\min}^2$$

or

$$\sigma_{\max}\|x_1\| \geq \|x_n\| \geq \sigma_{\min}\|x_1\|$$

The upper and lower bounds are reached when x_1 takes the values e_1 and e_2, respectively. Hence, taking the natural logarithm, dividing by $n-1$, and taking the limit as $n \to \infty$ results in

$$\lim_{n\to\infty} \frac{1}{n-1} \ln \sigma_{\max} \geq \lim_{n\to\infty} \frac{1}{n-1} \ln \|x_n\| \geq \lim_{n\to\infty} \frac{1}{n-1} \ln \sigma_{\min}$$

The larger Lyapunov exponent is then given by

$$\lambda_1 = \lambda_{\max} = \lim_{n\to\infty} \frac{1}{n-1} \ln \sigma_{\max} \tag{8}$$

From the well-known multiplicative ergodic theorem of Oseledec,[13] $\|x_n\|$ grows exponentially at the average rate $\lambda_{\max}$ for any x_1 except when $x_1 = e_2$. When $x_1 = e_2$, $\|x_n\|$ grows at the rate

$$\lambda_2 = \lambda_{\min} = \lim_{n\to\infty} \frac{1}{n-1} \ln \sigma_{\min} \tag{9}$$

It may be noted that $\lambda_2 = -\lambda_1$, since the determinant of matrix $B_n^T B_n$ is unity.

If a monocoupled structure is perfectly periodic, $T_2 = T_3 = \cdots = T_n = T$. Let Λ_1, Λ_2 ($|\Lambda_1| \geq |\Lambda_2|$) be the eigenvalues of T, and E_1, E_2 the corresponding orthonormal eigenvectors. It can be shown that $\sigma_{\max}^2 = |\Lambda_1|^{2n-2}$, $\sigma_{\min}^2 = |\Lambda_2|^{2n-2}$ are the eigenvalues of $B_n^T B_n$. Hence, from Eqs. (8) and (9), for any x_1, not parallel to E_2, $\|x_n\|$ grows exponentially at the rate $\lambda_1 = \ln|\Lambda_1|$, whereas when x_1 is parallel to E_2, $\|x_n\|$ grows exponentially at the rate $\lambda_2 = \ln|\Lambda_2|$.

If the multispan continuous beam shown in Fig. 1 is perfectly periodic, i.e., $L_1 = L_2 = \cdots = L_N = L$, $k_1 = k_2 = \cdots = k_N = k$, $t_1 = t_2 = \cdots = t_{N+1} = t$, the transfer matrix given by Eq. (2) is then

$$T = \begin{bmatrix} 2\gamma & -1 \\ 1 & 0 \end{bmatrix}, \quad \gamma = -\frac{1}{c}\left(1 + \frac{t}{2s}\right)$$

If $|\mathrm{tr}(T)| < 2$, i.e., $|\gamma| < 1$, the eigenvalues of T are complex and the Lyapunov exponents are $\lambda_{1,2} = 0$. For the values of axial compressive load P corresponding to $|\gamma| < 1$, buckling can occur. These ranges are known as the pass bands.

If $|\mathrm{tr}(T)| > 2$, i.e., $|\gamma| > 1$, the eigenvalues of T are real and $\|x_n\|$ grows exponentially at the rate

$$\lambda = \begin{cases} \mathrm{sgn}(\gamma) \ln\left|\gamma + \sqrt{\gamma^2 - 1}\right|, & \text{if } \theta_2/\theta_1 \neq \gamma - \mathrm{sgn}(\gamma)\sqrt{\gamma^2-1} \\ -\mathrm{sgn}(\gamma) \ln\left|\gamma + \sqrt{\gamma^2 - 1}\right|, & \text{if } \theta_2/\theta_1 = \gamma - \mathrm{sgn}(\gamma)\sqrt{\gamma^2-1} \end{cases} \tag{10}$$

For the values of axial load P corresponding to $|\gamma| > 1$, the larger Lyapunov exponent is positive and, therefore, buckling cannot occur. These regions are known as the stop bands.

When the structures are randomly disordered, the transfer matrices $T_2, T_3, \ldots, T_n$ are random matrices. The Lyapunov exponents or the localization factors λ can be easily determined using the following algorithm.

An arbitrary nonzero unit vector $\hat{x}_1$ is chosen first. The state vector x_i is determined iteratively. At the ith iteration

$$x_i = T_i \hat{x}_{i-1} \tag{11}$$

x_i is then normalized to give $x_i = \|x_i\| \hat{x}_i$. It is easy to show that

$$\|T_n T_{n-1} \cdots T_2 \hat{x}_1\| = \prod_{i=2}^{n} \|x_i\|$$

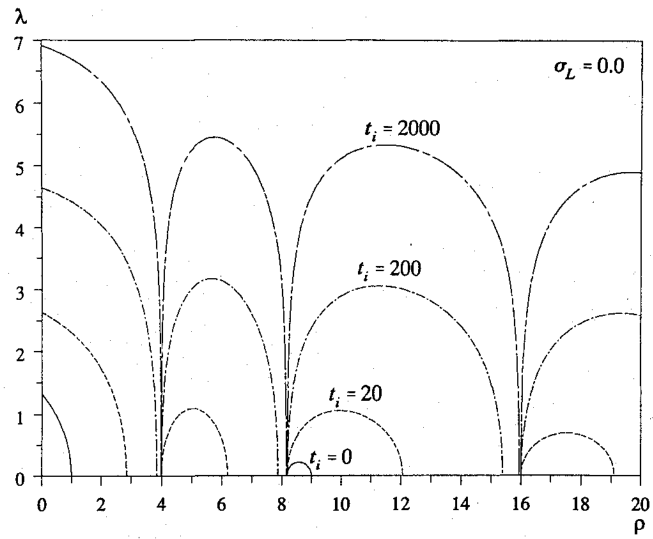

Fig. 3 Localization factors, period structure, $\sigma_L = 0.0$.

From Eq. (4), the Lyapunov exponent or the localization factor is obtained as

$$\lambda = \lim_{n\to\infty} \frac{1}{n-1} \sum_{i=2}^{n} \ln \|x_i\| \tag{12}$$

For perfectly periodic multispan continuous beams, the Lyapunov exponents or localization factors λ are calculated by Eq. (10) and are plotted in Fig. 3 for different values of the nondimensional torsional spring stiffness t. The pass bands are determined by $|\mathrm{tr}(T)| \leq 2$. The values of ρ corresponding to the upper ends of the pass bands are given by $1/s = 0$ and $c = -1$ for odd number pass bands or $c = 1$ for even number pass bands. The values of ρ corresponding to the lower ends of the pass bands are given by the roots of $|[1 + t/(2s)]/c| = 1$, in which $1/s \neq 0$. It is seen that the larger the value of the nondimensional torsional spring stiffness t or the weaker the coupling between the adjacent spans the smaller the width of the pass bands. As an extreme case, when t approaches infinity, the widths of the pass bands become zero; the pass bands are pass points. The pass bands corresponding to different values of t have the same upper-end value P or ρ, since the corresponding buckling modes have zero slope at all of the supports and the torsional springs do not affect the buckling of the multispan continuous beam.

As an example of disordered periodic structures, the lengths of the spans are assumed to be uniformly distributed random numbers with a mean value L and a standard deviation ρ_L, whereas other parameters are constants. Equation (12) is employed to determine the Lyapunov exponents or the localization factors numerically. In performing the simulation, for the ith iteration, a standard uniformly distributed random number R_i is generated, the length of the ith span is calculated as $L_i = L(1 + \sigma_L R_i)$, and the entries of the transfer matrix are calculated by Eq. (2). Iteration is carried out for a large number of transfer matrices, e.g., $n = 10^5$. Numerical results are plotted in Fig. 4 for $\sigma_L = 0.01$ and Fig. 5 for $\sigma_L = 0.1$ and different values of t_i. It can be seen that when $t_i = 0$, i.e., when the adjacent spans are strongly coupled, the localization factors are very small and localization in the buckling modes is weak. However, if t_i is large or if the adjacent spans are weakly coupled, the localization factors are large, especially when ρ is close to the ends of pass bands, which means that localization in the corresponding buckling modes is strong. At the middle of pass band, the localization factors are relatively small and localization in the buckling modes is relatively weak. From Figs. 4 and 5, it is also seen that the larger the disorder in the periodicity of the structure, the larger the degrees of localization in the buckling modes.

III. Buckling Mode Localization in Multispan Beams with Nonuniform Cross Sections

When the cross sections in each span of the N-span continuous beam are not uniform, the exact formulation used in Sec. II is not

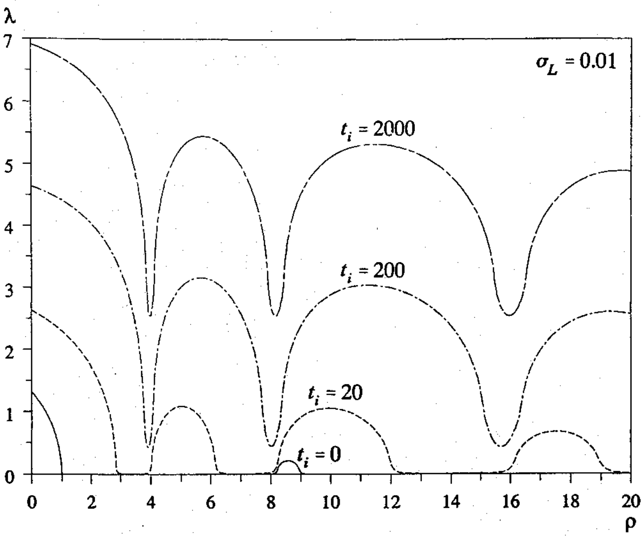

Fig. 4 Localization factors, disordered structure, σ_L = 0.01.

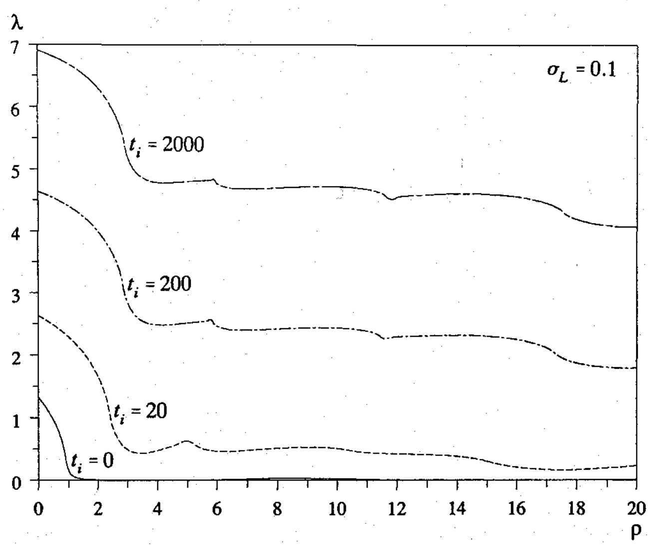

Fig. 5 Localization factors, disordered structure, σ_L = 0.1.

applicable; an approximate formulation has to be employed. In this section, the equations of equilibrium of the multispan beam are established by a finite element method.

Each span of the multispan beam is divided into M finite elements. A two-node beam element has four degrees of freedom, i.e., two translational displacements v_1^e and v_3^e, and two rotational displacements v_2^e and v_4^e (Fig. 6). Hence, each span has $2M - 1$ degrees of freedom as shown in Fig. 7, with the global degrees of freedom marked at each node. Each element of the beam is assumed to have a uniform cross section; the length and the flexural rigidity of the jth element in the ith span are L_{ij} and EI_{ij}, respectively.

The stiffness matrix of a two-node element as shown in Fig. 6 is given by

$$\boldsymbol{K}_{ij}^e = \frac{2EI_{ij}}{L_{ij}^3}\begin{bmatrix} 6 & 3L_{ij} & -6 & 3L_{ij} \\ 3L_{ij} & 2L_{ij}^2 & -3L_{ij} & L_{ij}^2 \\ -6 & -3L_{ij} & 6 & -3L_{ij} \\ 3L_{ij} & L_{ij}^2 & -3L_{ij} & 2L_{ij}^2 \end{bmatrix} \tag{13}$$

whereas the geometric stiffness matrix under axial compressive load P is

$$\boldsymbol{K}_{ij}^{G,e} = \frac{P}{30L_{ij}}\begin{bmatrix} 36 & 3L_{ij} & -36 & 3L_{ij} \\ 3L_{ij} & 4L_{ij}^2 & -3L_{ij} & -L_{ij}^2 \\ -36 & -3L_{ij} & 36 & -3L_{ij} \\ 3L_{ij} & -L_{ij}^2 & -3L_{ij} & 4L_{ij}^2 \end{bmatrix} \tag{14}$$

where the superscript e denotes element.

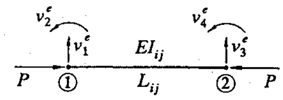

Fig. 6 Two-node beam element.

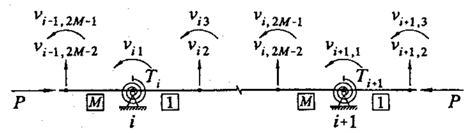

Fig. 7 Global coordinates of a multispan beam.

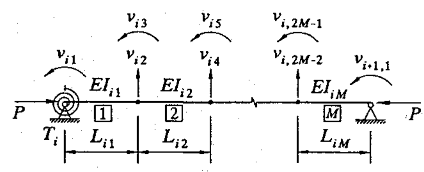

Fig. 8 *M*-element span.

For the span i as shown in Fig. 8, let the displacement vector be $\boldsymbol{v}_i^s = \{\boldsymbol{v}_{i1}^T, \boldsymbol{v}_{i2}^T, \ldots, \boldsymbol{v}_{iM}^T, \boldsymbol{v}_{i,M+1}^T\}^T$, where $\boldsymbol{v}_{i1}^T = \{v_{i1}\}$, $\boldsymbol{v}_{ij}^T = \{v_{i,2j-2}, v_{i,2j-1}\}$, $j = 2, 3, \ldots, M$, and $\boldsymbol{v}_{i,M+1}^T = \{v_{i+1,1}\}$. By assembling the element stiffness matrix (13) and the element geometric stiffness matrix (14), one obtains the stiffness matrix $\tilde{\boldsymbol{K}}_i^s$ and the geometric stiffness matrix $\tilde{\boldsymbol{K}}_i^{G,s}$ for span i, in which the superscript s stands for span. The equations of equilibrium are then given by

$$\left(\tilde{\boldsymbol{K}}_i^s - \tilde{\boldsymbol{K}}_i^{G,s}\right)\boldsymbol{v}_i^s = \boldsymbol{0} \tag{15}$$

Employing the following notation

$$u_{i1} = v_{i1}, \quad u_{i,2j-2} = v_{i,2j-2}/l, \quad u_{i,2j-1} = v_{i,2j-1}$$

$$j = 2, 3, \ldots, M, \quad u_{i+1,1} = v_{i+1,1}$$

and dividing equations $1, 3, \ldots, 2M - 1$, and $2M$ of Eq. (15) by $l^2 P_E$, and equations $2, 4, \ldots, 2M - 2$ of Eq. (15) by lP_E results in

$$\left(\boldsymbol{K}_i^s - \nu \boldsymbol{K}_i^{G,s}\right)\boldsymbol{u}_i^s = \boldsymbol{0} \tag{16}$$

where $\boldsymbol{u}_i^s = \{\boldsymbol{u}_{i1}^T, \boldsymbol{u}_{i2}^T, \ldots, \boldsymbol{u}_{iM}^T, \boldsymbol{u}_{i,M+1}^T\}^T$, $\boldsymbol{u}_{i1}^T = \{u_{i1}\}$, $\boldsymbol{u}_{ij}^T = \{u_{i,2j-2}, u_{i,2j-1}\}$, $j = 2, 3, \ldots, M$, $\boldsymbol{u}_{i,M+1}^T = \{u_{i+1,1}\}$, $\boldsymbol{K}_i^s$ and $\boldsymbol{K}_i^{G,s}$ are the nondimensional stiffness and geometric stiffness matrices for span i respectively given by

$$\boldsymbol{K}_i^s = \begin{bmatrix} \boldsymbol{K}_{i1}^s & (\boldsymbol{k}_{i1}^s)^T & & \cdots & \boldsymbol{0} \\ \boldsymbol{k}_{i1}^s & \boldsymbol{K}_{i2}^s & (\boldsymbol{k}_{i2}^s)^T & & \vdots \\ & \ddots & \ddots & \ddots & \\ \vdots & & \boldsymbol{k}_{i,M-1}^s & \boldsymbol{K}_{iM}^s & (\boldsymbol{k}_{iM}^s)^T \\ \boldsymbol{0} & \cdots & & \boldsymbol{k}_{iM}^s & \boldsymbol{K}_{i,M+1}^s \end{bmatrix} \tag{17}$$

$$\boldsymbol{K}_i^{G,s} = \begin{bmatrix} \boldsymbol{K}_{i1}^{G,s} & (\boldsymbol{k}_{i1}^{G,s})^T & & \cdots & \boldsymbol{0} \\ \boldsymbol{k}_{i1}^{G,s} & \boldsymbol{K}_{i2}^{G,s} & (\boldsymbol{k}_{i2}^{G,s})^T & & \vdots \\ & \ddots & \ddots & \ddots & \\ \vdots & & \boldsymbol{k}_{i,M-1}^{G,s} & \boldsymbol{K}_{iM}^{G,s} & (\boldsymbol{k}_{iM}^{G,s})^T \\ \boldsymbol{0} & \cdots & & \boldsymbol{k}_{iM}^{G,s} & \boldsymbol{K}_{i,M+1}^{G,s} \end{bmatrix} \tag{18}$$

the elements of $\boldsymbol{K}_i^s$ and $\boldsymbol{K}_i^{G,s}$ are given in the Appendix. Equation (16) may also be written as

$$\boldsymbol{A}_i^s \boldsymbol{u}_i^s = \boldsymbol{0} \tag{19}$$

where $\boldsymbol{A}_i^s = \boldsymbol{K}_i^s - \nu \boldsymbol{K}_i^{G,s}$.

For the span considered, $\boldsymbol{u}_i^B = \{u_{i1}, u_{i+1,1}\}^T$ are boundary degrees of freedom, and $\boldsymbol{u}_i^I = \{u_{i2}, u_{i3}, \ldots, u_{i,2M-1}\}^T$ are interior degrees of freedom. Using the method of condensation, the interior degrees of freedom may be expressed in terms of the boundary degrees of freedom. Equation (19) can be rearranged as

$$\begin{bmatrix} A_i^{BB} & A_i^{BI} \\ A_i^{IB} & A_i^{II} \end{bmatrix} \begin{Bmatrix} u_i^B \\ u_i^I \end{Bmatrix} = 0 \tag{20}$$

or

$$A_i^{BB} u_i^B + A_i^{BI} u_i^I = 0 \tag{21}$$

$$A_i^{IB} u_i^B + A_i^{II} u_i^I = 0 \tag{22}$$

From Eq. (22), u_i^I may be expressed in terms of u_i^B, for nonsingular A_i^{II}, $u_i^I = -(A_i^{II})^{-1} A_i^{IB} u_i^B$. Substituting u_i^I into Eq. (21) yields

$$A_i^B u_i^B = 0 \tag{23}$$

where A_i^B is a 2×2 symmetric matrix given by

$$A_i^B = A_i^{BB} - A_i^{BI}\left(A_i^{II}\right)^{-1} A_i^{IB} = \begin{bmatrix} \alpha_{i1} & \beta_i \\ \beta_i & \alpha_{i2} \end{bmatrix} \tag{24}$$

To compare with the exact results obtained in Sec. II, in the following numerical examples the M elements in each span are taken to be identical, i.e., $\kappa_{i1} = \kappa_{i2} = \cdots = \kappa_{iM} = \kappa_i$, $l_{i1} = l_{i2} = \cdots = l_{iM} = l_i$, and $r_{i1} = r_{i2} = \cdots = r_{iM} = r_i$. The elements of matrix A_i^B are

$$\alpha_{i1} = \alpha_{i2} + t_i/M, \quad \alpha_{i2} = [2(\kappa_i - 2\nu_i) + N_\alpha/D]\, l_i^2$$

$$\beta_i = N_\beta l_i^2/D$$

where $\nu_i = \nu r_i$, and for a two-element span, i.e., $M = 2$,

$$N_\alpha = 2\left(3\nu_i^3 - \kappa_i\nu_i^2 + 4\kappa_i^2\nu_i - \kappa_i^3\right)$$

$$N_\beta = \kappa_i\left(13\nu_i^2 - 4\kappa_i\nu_i + \kappa_i^2\right)$$

$$D = 2(6\nu_i - \kappa_i)(2\nu_i - \kappa_i)$$

whereas for a four-element span, i.e., $M = 4$,

$$N_\alpha = 3\big(11475\nu_i^7 - 24330\kappa_i\nu_i^6 + 32890\kappa_i^2\nu_i^5 - 27248\kappa_i^3\nu_i^4 + 11123\kappa_i^4\nu_i^3 - 2066\kappa_i^5\nu_i^2 + 160\kappa_i^6\nu_i - 4\kappa_i\big)$$

$$N_\beta = -\big(10125\nu_i^7 - 33300\kappa_i\nu_i^6 + 37590\kappa_i^2\nu_i^5 - 21818\kappa_i^3\nu_i^4 + 6301\kappa_i^4\nu_i^3 - 960\kappa_i^5\nu_i^2 + 64\kappa_i^6\nu_i - 2\kappa_i\big)$$

$$D = 8(6\nu_i - \kappa_i)\big(2025\nu_i^5 - 3645\kappa_i\nu_i^4 + 2195\kappa_i^2\nu_i^3 - 516\kappa_i^3\nu_i^2 + 42\kappa_i^4\nu_i - \kappa_i^5\big)$$

For the N-span beam as shown in Fig. 1, assembling Eqs. (24) gives the equations of equilibrium

$$\begin{bmatrix} \alpha_1 & \beta_1 & & \cdots & 0 \\ \beta_1 & \alpha_2 & \beta_2 & & \vdots \\ & \ddots & \ddots & \ddots & \\ \vdots & & \beta_{N-1} & \alpha_N & \beta_N \\ 0 & \cdots & & \beta_N & \alpha_{N+1} \end{bmatrix} \begin{Bmatrix} \theta_1 \\ \theta_2 \\ \vdots \\ \theta_N \\ \theta_{N+1} \end{Bmatrix} = 0 \tag{25}$$

where $\alpha_1 = \alpha_{11}$, $\alpha_i = \alpha_{i-1,2} + \alpha_{i1}$, $i = 2, 3, \ldots, N$, $\alpha_{N+1} = \alpha_{N2} + t_{N+1}/M$, and $\theta_i = u_{i1}$, $i = 1, 2, \ldots, N+1$.

In the following, localization in the buckling modes is studied; the method of transfer matrix and the method of Green's function are applied to determine the localization factors.

Method of Transfer Matrix

Equations (25) may be written in the form of difference equations

$$\beta_{i-1}\theta_{i-1} + \alpha_i\theta_i + \beta_i\theta_{i+1} = 0 \tag{26}$$

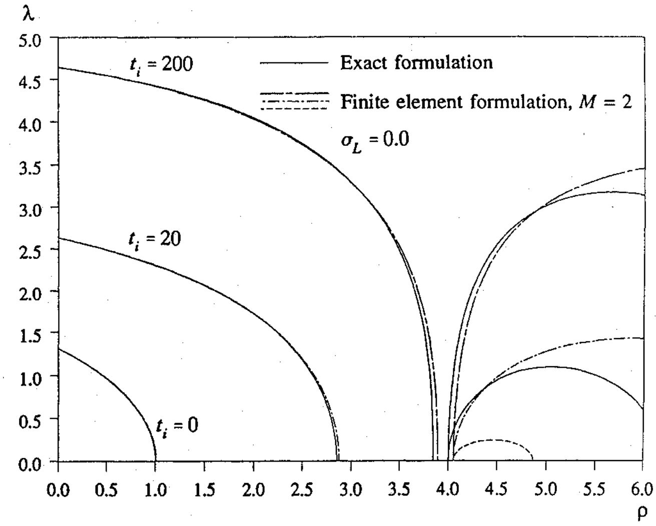

Fig. 9 Localization factors, period structure, σ_L = 0.0.

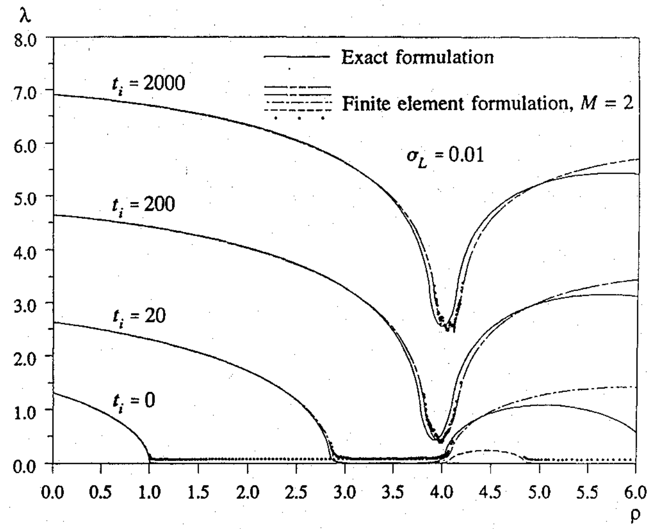

Fig. 10 Localization factors, disordered structure, σ_L = 0.01.

From Eq. (26), one obtains

$$x_i = T_i x_{i-1}, \quad x_i = \begin{Bmatrix} \theta_{i+1} \\ \theta_i \end{Bmatrix}, \quad T_i = \begin{bmatrix} -\dfrac{\alpha_i}{\beta_i} & -\dfrac{\beta_{i-1}}{\beta_i} \\ 1 & 0 \end{bmatrix} \tag{27}$$

Equations (2) and (27) are of the same form; the only differences are the entries of the transfer matrices T_i. Hence, the method employed in Sec. II may be used to determine the localization factors for the buckling modes. As in Sec. II, the length of each span is assumed to be a uniformly distributed random number with a mean value L and a standard deviation σ_L, whereas other parameters are constants.

If only two finite elements are taken for each span, the buckling loads in the first pass bands are reasonably accurate. The Lyapunov exponents or the localization factors for $\sigma_L = 0.0$, 0.01, and 0.1 and different values of t_i are plotted in Figs. 9–11 in broken lines.

When more finite elements are taken for each span, the buckling loads in the higher pass bands are more accurate. In Figs. 12–14, the localization factors obtained for four-element spans are shown in broken lines.The exact results obtained in Sec. II are also plotted in Figs. 9–14 in solid lines for the purpose of comparison. It is seen that, when four elements are taken for each span, the buckling loads in the first two pass bands are quite accurate. The accuracy of approximation can be improved by increasing the number of finite elements for each span. The numerical results obtained from a finite element formulation are seen to agree quite well with those obtained from an exact formulation. Hence, the method of finite element presented in this section is suitable for studying the localization phenomenon in buckling modes of multispan beams with nonuniform cross sections.

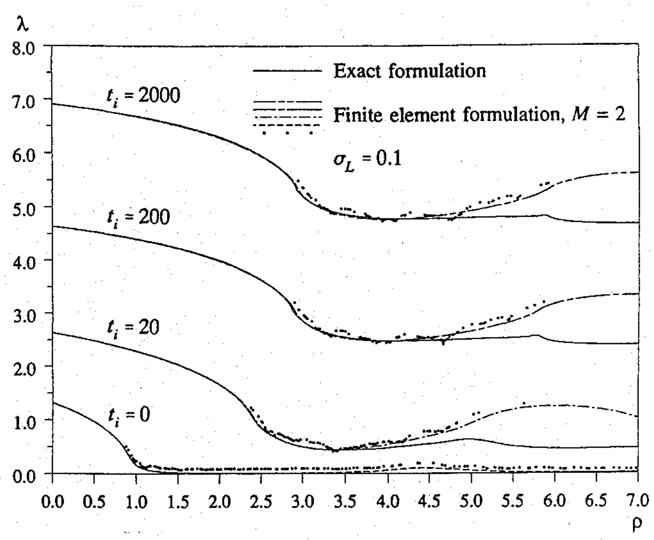

Fig. 11 Localization factors, disordered structure, σ_L = 0.1.

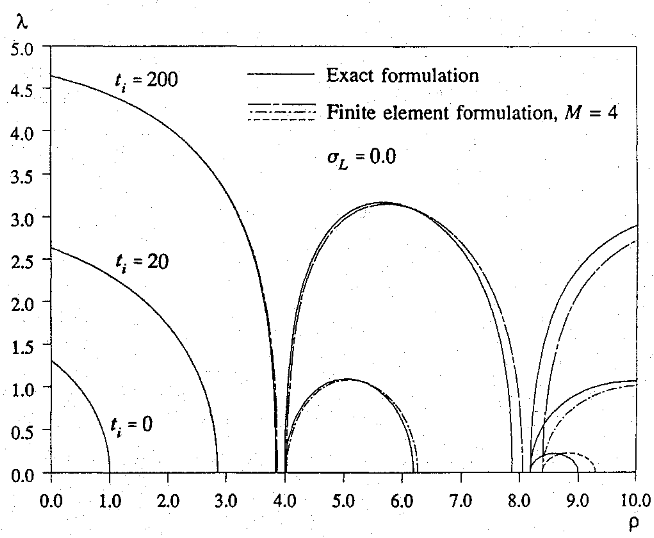

Fig. 12 Localization factors, period structure, σ_L = 0.0.

Method of Green's Function

Green's function formulation has been applied by Thouless[4] to determine the localization factor for one-dimensional disordered systems, where the governing equations form a tridiagonal system. Using the method of Green's function to calculate the localization factors involves the eigenvalues and eigenvectors.

If the method of condensation is applied in the formulation, namely, Eqs. (23) are employed to set up the equations of equilibrium of the N-span continuous beam, the governing equations are in terms of the angles of rotation at the supports. Although the matrix is of a tridiagonal form, the stability problem is a nonlinear eigenvalue problem (25), which is very difficult to handle even numerically. On the other hand, when both the boundary and interior degrees of freedom are used to establish the equations of equilibrium, i.e., Eqs. (19) are employed, one obtains a linear eigenvalue problem of a block tridiagonal form. A linear eigenvalue problem is easier to study and is, therefore, suitable for determining the localization factors using Green's function formulation.

Assembling Eqs. (19) for the N-span continuous beam leads to the equations of equilibrium

$$(\nu \boldsymbol{K}^G - \boldsymbol{K})\boldsymbol{u} = \boldsymbol{0} \tag{28}$$

The elements of the block tridiagonal matrices $\boldsymbol{K}$, $\boldsymbol{K}^G$, and the displacements vector $\boldsymbol{u}$ are given in the Appendix. For system (28), Green's functions $\boldsymbol{G}_{ij}$ are defined by

$$\left(\nu \boldsymbol{k}_{i-1}^G - \boldsymbol{k}_{i-1}\right)\boldsymbol{G}_{i-1,j} + \left(\nu \boldsymbol{K}_i^G - \boldsymbol{K}_i\right)\boldsymbol{G}_{ij} + \left[\nu\left(\boldsymbol{k}_i^G\right)^T - \boldsymbol{k}_i^T\right]\mathbf{G}_{i+1,j} = \delta_{ij}\boldsymbol{I} \tag{29}$$

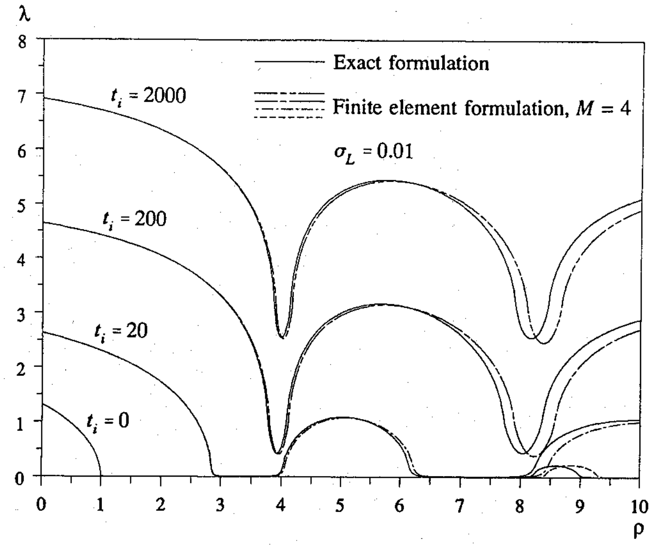

Fig. 13 Localization factors, disordered structure, σ_L = 0.01.

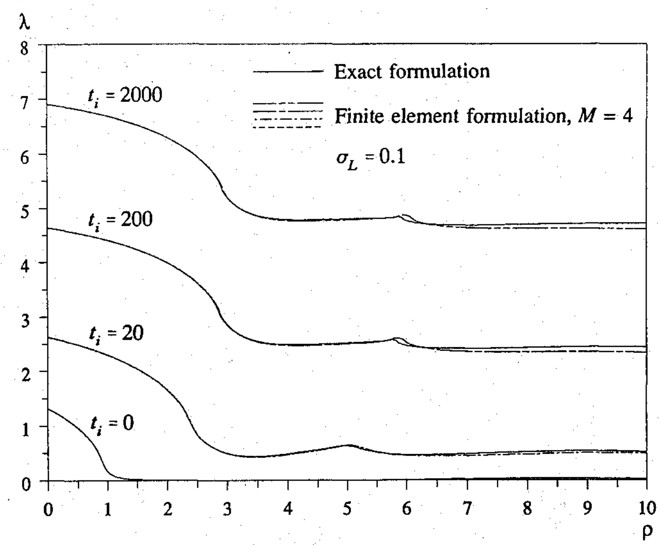

Fig. 14 Localization factors, disordered structure, σ_L = 0.1.

Green's functions can be expressed in terms of the eigenvalues and eigenvectors of the generalized eigenvalue problem (28).

Let $\{\nu_{11}, \ldots, \nu_{1,2M-1}; \nu_{21}, \ldots, \nu_{2,2M-1}; \ldots; \nu_{N1}, \ldots, \nu_{N,2M-1}; \nu_{N+1,1}\}$ be the eigenvalues of system (28) and the eigenvector corresponding to ν_{kl} be $\phi^{kl} = \{\phi_{11}^{kl}, \phi_{12}^{kl}, \ldots, \phi_{N,2M-1}^{kl}, \phi_{N+1,1}^{kl}\}^T$. It has been shown that the rsth element of Green's function $\boldsymbol{G}_{1N}$ is[14]

$$G_{1N}^{rs} = \sum_{k=1}^{N}\sum_{l=1}^{2M-1}\frac{\phi_{1r}^{kl}\phi_{Ns}^{kl}}{\nu - \nu_{kl}} + \frac{\phi_{1r}^{N+1,1}\phi_{Ns}^{N+1,1}}{\nu - \nu_{N+1,1}} \tag{30}$$

The residual of G_{1N}^{rs} at $\nu = \nu_{kl}$ is

$$\operatorname*{Res}_{\nu=\nu_{kl}} G_{1N}^{rs} = \lim_{\nu \to \nu_{kl}} (\nu - \nu_{kl})G_{1N}^{rs} = \phi_{1r}^{kl}\phi_{Ns}^{kl} \tag{31}$$

For the klth mode with eigenvalue ν_{kl}, $\boldsymbol{u}_1$ and $\boldsymbol{u}_N$ are the amplitudes of deformation at the 1st and the Nth spans, respectively. Hence,

$$\|\boldsymbol{u}_1\|^2 \cdot \|\boldsymbol{u}_N\|^2 = \sum_{r=1}^{2M-1}\sum_{s=1}^{2M-1}\left(\phi_{1r}^{kl}\phi_{Ns}^{kl}\right)^2 = \sum_{r=1}^{2M-1}\sum_{s=1}^{2M-1}\left(\operatorname*{Res}_{\nu=\nu_{kl}} G_{1N}^{rs}\right)^2 \tag{32}$$

Equation (32) may be used to determine whether or not the eigenvector (buckling mode) of the continuous beam is localized, since the $(N-1)$th root of $\|\boldsymbol{u}_1\| \cdot \|\boldsymbol{u}_N\|$ tends to unity as N tends to infinity for a nonlocalized eigenvector, whereas it tends to a constant less than unity, denoted by $\exp(-\lambda_{kl})$, for the localized klth eigenvector. Using the same argument as in Sec. II, if the klth buckling mode has its maximum at the ith span, $\|\boldsymbol{u}_1\|$, $\|\boldsymbol{u}_N\|$ should be of the orders $\exp\{-\lambda_{kl}(i-1)\}$ and $\exp\{-\lambda_{kl}(N-i)\}$, respectively, where λ_{kl} is the localization factor for the klth mode; hence, $\|\boldsymbol{u}_1\| \cdot \|\boldsymbol{u}_N\| = C\exp\{-\lambda_{kl}(N-1)\}$, where C is a constant. From Eq. (33),

$$\lambda_{kl} = \lim_{N\to\infty} \frac{1}{-2(N-1)} \log\left\{\sum_{r=1}^{2M-1}\sum_{s=1}^{2M-1}\left(\operatorname*{Res}_{\nu=\nu_{kl}} G_{1N}^{rs}\right)^2\right\} \tag{33}$$

The localization factor λ_{kl} for the klth buckling mode has thus been obtained in terms of the residual of Green's functions. The problem now remains to evaluate the residual of $\boldsymbol{G}_{1N}$ at $\nu = \nu_{kl}$. From the definition of Green's functions (29), one has

$$(\nu \boldsymbol{K}^G - \boldsymbol{K})\begin{bmatrix} \boldsymbol{G}_{1N} \\ \boldsymbol{G}_{2N} \\ \vdots \\ \boldsymbol{G}_{N+1,N} \end{bmatrix} = \begin{bmatrix} \boldsymbol{0} \\ \vdots \\ \boldsymbol{0} \\ \boldsymbol{I} \\ \boldsymbol{0} \end{bmatrix} \tag{34}$$

Using Kramer's rule, the rsth element of $\boldsymbol{G}_{1N}$ is obtained as $G_{1N}^{rs} = \Delta_{1N}^{rs}/\Delta$, where $\Delta = \det(\nu\boldsymbol{K}^G - \boldsymbol{K})$, and Δ_{1N}^{rs} is the determinant of the coefficient matrix when all of the elements of the rth column are set to 0 except the element at the $[(N-1)(2M-1)+s]$th row, which is set to 1.

Let $\boldsymbol{\Phi} = [\phi^{11}, \phi^{12}, \ldots, \phi^{N,2M-1}, \phi^{N+1,1}]$ be the modal matrix of the eigenvalue problem (28). Then

$$\Delta = [\det(\boldsymbol{\Phi})]^{-2} \prod_{i=1}^{N}\prod_{j=1}^{2M-1}(\nu - \nu_{ij})(\nu - \nu_{N+1,1}) \tag{35}$$

At $\nu = \nu_{kl}$,

$$\operatorname*{Res}_{\nu=\nu_{kl}} G_{1N}^{rs} = \lim_{\nu\to\nu_{kl}}(\nu-\nu_{kl})\frac{\Delta_{1N}^{rs}}{\Delta}$$

$$= [\det(\boldsymbol{\Phi})]^2 \Delta_{1N}^{rs}|_{\nu=\nu_{kl}} \prod_{\substack{n=1 \\ n\neq(k-1)(2M-1)+l}}^{N(2M-1)+1} [\nu_{(k-1)(2M-1)+l} - \nu_n]^{-1} \tag{36}$$

where, in the denominator, the eigenvalues have been renumbered as $\nu_1, \nu_2, \ldots, \nu_{N(2M-1)+1}$. Using Eqs. (33) and (36), the localization factor for the klth mode can be evaluated numerically.

Numerical analysis was performed to calculate the localization factors of buckling modes for a multispan continuous beam. A disordered 100-span continuous beam is considered, in which two identical elements are taken for each span for simplicity of illustration. The length of each span is again assumed to be a uniformly distributed random number with mean value L and standard deviation σ_L, whereas other parameters are assumed to be constants. Equations (33) and (36) are applied to evaluate the localization factors; for the purpose of comparison, numerical results are shown in Figs. 10 and 11 as solid dots for $\sigma_L = 0.01$ and 0.1, respectively. It can be seen that the results obtained by using Green's functions and those by using transfer matrices agree very well. To determine the localization factor of a specific finite multispan beam, the method of Green's function gives a more accurate result, since both the eigenvalues and eigenvectors are utilized. The method gives the buckling modes as well. However, to determine the localization factors of a large randomly disordered multispan beam, the method of transfer matrix is more efficient than the method of Green's function, since the latter involves an eigenvalue problem of large dimension.

The first five buckling modes of a randomly disordered 100-span beam are shown in Fig. 15 for $\sigma_L = 0.01$, $t_i = 20$, and $M = 2$. The exponential growth (decay) of the amplitudes of the buckling mode $\|\boldsymbol{u}_i\|$ can be easily observed when they are plotted in the logarithmic scale (Fig. 16).

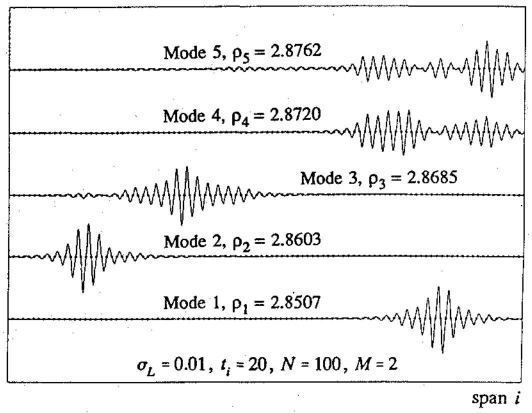

Fig. 15 Buckling modes, disordered structure, σ_L = 0.01.

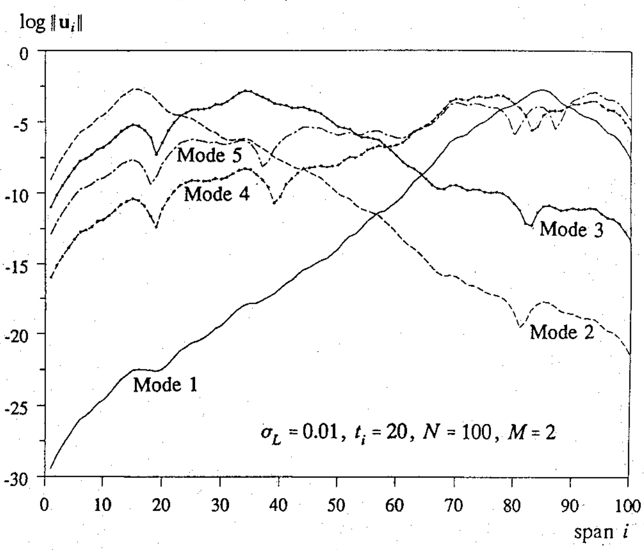

Fig. 16 Buckling modes, disordered structure, σ_L = 0.01.

IV. Conclusions

The buckling mode localization in large randomly disordered multispan continuous beams under compressive axial load was investigated. When the cross sections within each span are uniform, an exact formulation was employed to establish the equations of equilibrium. If the cross sections within a span are not uniform, there is no exact formulation available; a finite element method was applied to set up the governing equations. The equations of equilibrium can be expressed in the form of transfer matrices. Since the structure is monocoupled, the deformations of the structure can be determined by the angles of rotation at the supports; the dimension of the transfer matrices is 2 × 2. Furstenberg's theorem on the limiting behavior of products of random matrices was employed to determine the Lyapunov exponent or the localization factor. The positivity of the Lyapunov exponent for disordered structures leads to the localization in buckling modes. The second approach applied the method of Green's function for block tridiagonal system to determine the localization factors. The drawback of this method is that, when the number of finite elements is increased, the size of the matrices involved becomes very large and, hence, may create a computational problem.

A torsional spring has been used at each support to simulate the coupling between the adjacent spans. If the multispan beam is disordered, the localization factors are always positive, implying localization in the buckling modes. When the adjacent spans are strongly coupled, the localization factors are small and localization in the buckling modes is weak. If the adjacent spans are weakly coupled, the localization factors are large, especially when ρ is close to the ends of pass bands, which means that localization in the corresponding buckling modes is strong. At the middle of a pass band, the localization factors are relatively small and localization in the buckling modes is relatively weak. It was also seen that the larger the disorder in the periodicity of the structure, the larger the degrees of localization in buckling modes.

It is well known that, in an imperfect structure, any tiny perturbation or imperfection would be magnified by the factor $|1-P_n/P|^{-1}$, where P_n is the nth buckling load, which leads to nonzero deformation when P is close to P_n. The positivity of the Lyapunov exponent implies that the deformation is of a localized shape. Hence, there is localized deformation of a large randomly disordered imperfect structure under a compressive axial load P which is close to any of the buckling loads. Thus, for large randomly disordered multispan beams, the buckling mode will be localized when the compressive axial load is equal to one of the buckling loads. For an arbitrary value of compressive axial load close to the buckling loads, the deformation will be localized if there exist perturbations or imperfections. This behavior may be used to explain the existence of bulges (localized buckling modes) in long stiffened tubes or large stiffened plates or shells when subjected to compressive load.

Even though this paper dealt with one-dimensional randomly disordered multispan continuous beams, the principle and results can be extended to two- and three-dimensional structures such as stiffened plates and shells, in which only localized modes were observed in buckling experiments.

Appendix

Elements of Matrices K_i^s and $K_i^{G,s}$

$$K_{i1}^s = \left[2\kappa_{i1}l_{i1}^2 + t_i/M\right], \qquad K_{i,M+1}^s = \left[2\kappa_{iM}l_{iM}^2\right]$$

$$K_{ij}^s = \begin{bmatrix} 6(\kappa_{i,j-1}+\kappa_{ij}) & -3(\kappa_{i,j-1}l_{i,j-1}-\kappa_{ij}l_{ij}) \\ -3(\kappa_{i,j-1}l_{i,j-1}-\kappa_{ij}l_{ij}) & 2\left(\kappa_{i,j-1}l_{i,j-1}^2+\kappa_{ij}l_{ij}^2\right) \end{bmatrix}$$

$$j = 2, 3, \ldots, M$$

$$k_{i1}^s = \kappa_{i1}l_{i1}\begin{bmatrix} -3 \\ l_{i1} \end{bmatrix}, \qquad k_{iM}^s = \kappa_{iM}l_{iM}[3 \quad l_{iM}]$$

$$k_{ij}^s = \kappa_{ij}\begin{bmatrix} -6 & -3l_{ij} \\ 3l_{ij} & l_{ij}^2 \end{bmatrix}, \qquad j = 2, 3, \ldots, M-1$$

$$K_{i1}^{G,s} = [4l_{i1}], \qquad K_{i,M+1}^{G,s} = [4l_{iM}]$$

$$K_{ij}^{G,s} = \begin{bmatrix} 36(r_{i,j-1}+r_{ij}) & 0 \\ 0 & 4(l_{i,j-1}+l_{ij}) \end{bmatrix}, \qquad j = 2, 3, \ldots, M$$

$$k_{i1}^{G,s} = \begin{bmatrix} -3 \\ -l_{i1} \end{bmatrix}, \qquad k_{iM}^{G,s} = [3 \quad -l_{iM}]$$

$$k_{ij}^{G,s} = \begin{bmatrix} -36r_{ij} & -3 \\ 3 & -l_{ij} \end{bmatrix}, \qquad j = 2, 3, \ldots, M-1$$

Elements of K, K^G and u

Let $A = K - \nu K^G$. The elements of A or K and K^G can be expressed in terms of the elements of K_i^s and $K_i^{G,s}$. Hence,

$$A = \begin{bmatrix} A_1 & a_1^T & & \cdots & 0 \\ a_1 & A_2 & a_2^T & & \vdots \\ & \ddots & \ddots & \ddots & \\ \vdots & & a_{N-1} & A_N & a_N^T \\ 0 & \cdots & & a_N & A_{N+1} \end{bmatrix}, \qquad u = \begin{Bmatrix} u_1 \\ u_2 \\ \vdots \\ u_N \\ u_{N+1} \end{Bmatrix}$$

where $A_i = K_i - \nu K_i^G$, $a_i = k_i - \nu k_i^G$, and

$$A_i = \begin{bmatrix} A_{i-1,M+1}^s + A_{i1}^s & \left(a_{i1}^s\right)^T & & \cdots & 0 \\ a_{i1}^s & A_{i2}^s & \left(a_{i2}^s\right)^T & & \vdots \\ & \ddots & \ddots & \ddots & \\ \vdots & & a_{i,M-2}^s & A_{i,M-1}^s & \left(a_{i,M-1}^s\right)^T \\ 0 & \cdots & & a_{i,M-1}^s & A_{iM}^s \end{bmatrix}$$

$$u_i = \begin{Bmatrix} u_{i1} \\ u_{i2} \\ \vdots \\ u_{iM} \end{Bmatrix} = \begin{Bmatrix} u_{i1} \\ u_{i2} \\ \vdots \\ u_{i,2M-1} \end{Bmatrix}, \qquad i = 1, 2, \ldots, N$$

$$a_i = \begin{bmatrix} 0 & 0 & \ldots & 0 & a_{iM}^s \\ 0 & 0 & \ldots & 0 & 0 \\ \vdots & \vdots & \ldots & \vdots & \vdots \\ 0 & 0 & \ldots & 0 & 0 \end{bmatrix}, \qquad i = 1, 2, \ldots, N-1$$

$$A_{N+1} = \left[A_{N,M+1}^s + t_{N+1}/M\right], \qquad a_N = \left[0 \quad 0 \quad \ldots \quad 0 \quad a_{NM}^s\right]$$

$$u_{N+1} = \{u_{N+1,1}\}, \qquad A_{ij}^s = K_{ij}^s - \nu K_{ij}^{G,s}, \qquad a_{ij}^s = k_{ij}^s - \nu k_{ij}^{G,s}$$

Acknowledgment

The research for this paper was supported, in part, by the National Sciences and Engineering Research Council of Canada through Grant OGPO121355.

References

[1]Ishii, K., "Localization of Eigenstates and Transport Phenomena in the One-Dimensional Disordered System," *Supplement of the Progress of Theoretical Physics*, No. 53, 1973, pp. 77–138.

[2]Furstenberg, H., "Noncommuting Random Products," *Transactions of the American Mathematical Society*, Vol. 108, No. 3, 1963, pp. 377–428.

[3]Herbert, D. C., and Jones, R., "Localized States in Disordered Systems," *Journal of Physics C: Solid State Physics*, Vol. 4, No. 10, 1971, pp. 1145–1161.

[4]Thouless, D. J., "A Relation between the Density of States and Range of Localization of One Dimensional Random Systems," *Journal of Physics C: Solid State Physics*, Vol. 5, No. 1, 1972, pp. 77–81.

[5]Hodges, C. H., "Confinement of Vibration by Structural Irregularity," *Journal of Sound and Vibration*, Vol. 82, No. 3, 1982, pp. 411–424.

[6]Pierre, C., and Dowell, E. H., "Localization of Vibrations by Structural Irregularity," *Journal of Sound and Vibration*, Vol. 114, No. 3, 1987, pp. 549–564.

[7]Cha, P. D., and Pierre, C., "Vibration Localization by Disorder in Assemblies of Monocoupled, Multimode Component Systems," *Journal of Applied Mechanics*, Vol. 58, No. 4, 1991, pp. 1072–1081.

[8]Bouzit, D., and Pierre, C., "Vibration Confinement Phenomena in Disordered, Mono-Coupled, Multi-Span Beams," *Journal of Vibration and Acoustics*, Vol. 114, No. 4, 1992, pp. 521–530.

[9]Pierre, C., and Plaut, R. H., "Curve Veering and Mode Localization in a Buckling Problem," *Journal of Applied Mathematics and Physics (Zeitschrift für angewandte Mathematik und Physik)*, Vol. 40, 1989, pp. 758–761.

[10]Singer, J., "The Influence of Stiffener Geometry and Spacing on the Buckling of Axially Compressed Cylindrical and Conical Shells," *Theory of Thin Shells*, edited by F. I. Niordson, International Union of Theoretical and Applied Mechanics (IUTAM) Second Symposium (Copenhagen, Denmark), Springer–Verlag, Berlin, 1969, pp. 234–263.

[11]Tenerelli, D. J., and Horton, W. H., "An Experimental Study of the Local Buckling of Ring-Stiffened Cylinders Subject to Axial Compression," *Israel Journal of Technology*, Vol. 7, No. 1–2, 1969, pp. 181–194.

[12]Horne, M. R., and Merchant, W., *The Stability of Frames*, Pergamon, Oxford, England, UK, 1965.

[13]Oseledec, Y. I., "A Multiplicative Ergodic Theorem. Lyapunov Characteristic Number for Dynamical Systems," *Transactions of the Moscow Mathematical Society*, Vol. 19, 1968, pp. 197–231 (English translation).

[14]Xie, W.-C., and Zhang, Y., "Vibration Mode Localization in Disordered Large Planar Lattice Trusses" (to be published).